Flux noise resulting from vortex avalanches using a simple kinetic model

G. Mohler and D. Stroud
Department of Physics, The Ohio State University, Columbus, Ohio 43210
(Received 15 April 1999)

We have carried out a model calculation of the flux noise produced by vortex avalanches in a type-II superconductor, using a simple kinetic model proposed by Bassler and Paczuski. Over a broad range of frequencies, we find that the flux noise $S_\Phi(\omega)$ has a power-law dependence on frequency, $S_\Phi(\omega) \sim \omega^{-s}$, with $s \sim 1.4$ in reasonable agreement with experiment. In addition, for small lattices, the calculated $S_\Phi(\omega)$ has a high-frequency knee, which is seen in some experiments, and which is due to the finite lattice size. Deviations between calculation and experiment are attributed mostly to uncertainties in the measured critical current densities and pinning strengths of the experimental samples. [S0163-1829(99)07037-X]

I. INTRODUCTION

Bassler and Paczuski[1] have recently proposed a model which simulates the development of the Bean critical state in a type-II superconductor, as well as of other types of so-called self-organized critical behavior.[2] In such a system, vortices are injected into one edge of an initially empty sample, and are free to fall off the opposite edge only. As vortices are driven into the system from the ''loading edge,'' they push already-present vortices further into the sample. These existing vortices then pile up in such a way that the vortex density gradient approaches a critical value which is determined by system parameters such as pinning strength and density. Once the gradient reaches this critical value, the system is said to have achieved a ''self-organized critical state.''

Of particular interest in this context, is the development of ''avalanches'' from the Bean critical state. When the flux density gradient exceeds its critical value, the injection of even a single excess vortex into the system can start a chain reaction of vortex motion, known as an avalanche, which may have a very large scale in both space and time and which causes the gradient to relax back to its critical value. Vortex avalanches are typically characterized by their duration, their linear extent in the direction of average vortex motion, and the number of vortices forced from their original positions (''topplings'') by the avalanche. These and other avalanche characteristics are expected to obey various scaling laws.[3]

In earlier numerical models, the generation of vortex avalanches was typically studied numerically at a ''microscopic'' scale, i.e., at a length scale where individual vortex displacements were calculated from certain postulated force laws.[4] In practice, this type of model imposes severe constraints on the size of system which can be studied numerically; such constraints in turn make it difficult to study the critical behavior of vortex avalanches. But since an avalanching system is expected eventually to achieve a self-organized critical state, the large-scale behavior of the system should be describable without tracking the motion of individual vortices. The BP model takes advantage of this expectation by focusing attention only on the large-length scale behavior of this system, which can be modeled using only a coarse-grained lattice. This choice makes feasible the simulation of large systems.

II. THE BASSLER-PACZUSKI MODEL: DEFINITION AND METHOD OF CALCULATION

In the Bassler-Paczuski (BP) model, one considers a distribution of vortices on a two-dimensional simple hexagonal lattice (see Fig. 1). The scale of the lattice is assumed to be such that the vortices can be treated as pointlike objects which exist entirely on the lattice sites. Each lattice site is capable of containing multiple vortices, and the number of vortices per lattice site is a kind of coarse-grained vortex density.[5] Each lattice site is also described by a pinning potential, which is chosen at random from a suitable distribution. Periodic boundary conditions are imposed at the top and bottom of the lattice. Vortices are injected into the left-hand edge, and removed from the right-hand edge, as described in more detail below. As more and more vortices are injected into the lattice, the repulsion between vortices eventually overcomes the attraction exerted on the vortices by the pinning sites. As a result, the vortices slowly migrate from

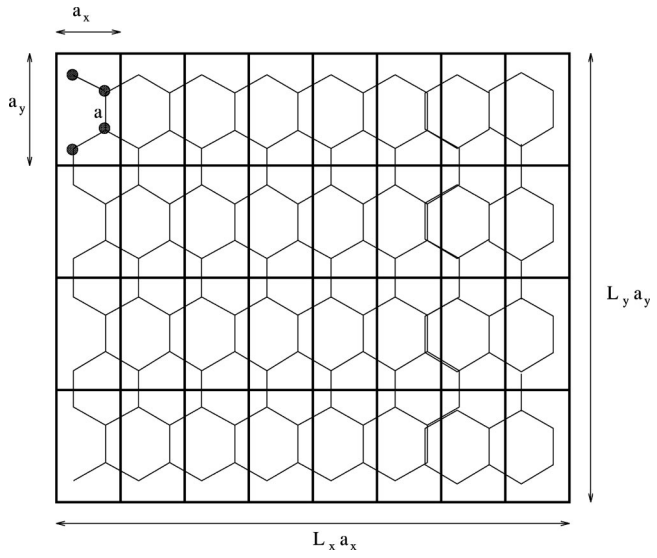

FIG. 1. Hexagonal lattice, with a rectangular overlay displaying the unit cells used in the calculations. Our ''unit cell'' is a rectangle enclosing four lattice points as shown.

 ©1999 The American Physical Society

left to right across the lattice. When they reach the right-hand edge, in this model, they are assumed to ''fall off'' the lattice and are removed from the system. Vortices are forbidden to exit from the left side of the system, or to re-enter the lattice from the right-hand side once they fall off.

An important parameter in the BP model is the rate of vortex injection. In the ''slow-driving limit,''[1] a vortex is injected into the lattice only after an avalanche has ceased. This slow-driving limit is similar to that studied in models which treat the microscopic (i.e., the individual vortex) degrees of freedom together with explicit force equations for each vortex. For example, Nori *et al.*,[4] who have studied such a model, introduce a new vortex into the lattice only when the lattice-averaged vortex velocity has fallen below a certain threshold. In the present paper, we inject vortices either slowly or quickly, so that we may make predictions for either a hypothetical slow-driving regime or the high magnetic field ramping rates studied in most experiments.[6]

In the BP model, the force acting on a vortex at site x in the direction of site y is taken to be

$$F_{x\to y} = -V(x)+V(y)+[m(x)-m(y)-1] + r[m(x1)+m(x2)-m(y1)-m(y2)]. \quad (1)$$

Here $x1$ and $x2$ are the two sites (other than site y) which neighbor x on the hexagonal lattice, $y1$ and $y2$ are the two sites other than x which are nearest neighbors to y, $V(z)$ is the strength of the pinning potential on site z, and $m(z)$ is the vortex population at site z (taken to be a positive integer). r is the strength of the repulsion between vortices on neighboring sites, in units such that the on-site repulsion strength is normalized to 1.

The BP model is defined by three parameters, denoted r, p, and q. r is the nearest-neighbor repulsion parameter mentioned above, which is assumed to be smaller than unity, p is the pinning strength, and q is the probability that a particular site contains a nonzero pinning potential. Thus, any particular site has a pinning strength of p or 0 with probability q and $1-q$, respectively. The distribution of pinning sites is determined at random once for the entire lattice, at the start of the simulation, and is held constant thereafter.

A vortex move is carried out as follows. First, the force on a vortex is calculated for each of the three possible directions of vortex motion. If exactly one of the three forces is greater than zero (i.e., acts towards a nearest neighbor site), then one vortex is moved by one lattice spacing in the direction of that force. If more than one force is greater than zero, the direction of motion is chosen randomly from the set of positive forces. This calculation is carried out for each site containing at least one vortex, and all the vortex populations are updated in parallel — that is, each site is examined once in a given time step, and at most one vortex is moved from a particular site during a time step.

To carry out the calculations, we constructed a simple hexagonal lattice using the unit cell shown in Fig. 1, with cell length a_x and cell height $a_y=\sqrt{3}a_x$. The total lattice size was chosen so as to have dimensions $L_x a_x \times L_y a_y$, as shown in the figure, with $L_x=4L_y$, and L_y integer. For this choice of dimensions, and for $L_x>32$, the rectangular sample was found to be wide enough to prevent individual avalanche events from overlapping one another in space. For a given lattice size, we carried out simulations of avalanche formation and evolution for a range of pinning strengths and vortex injection rates.

TABLE I. Calculated lattice constant a and magnetization density $m(0)$ for several lattice sizes and two choices of model parameters.

L	$m(0)(\Phi_0)$	$a(10^{-5}$ cm)	slope [a]
128[b]	7500	3.22	1.83
64[b]	1900	3.24	1.86
64[c]	2300	(3.45)	2.25
32[b]	510	3.37	1.99

[a]The slope is calculated from the columnar vortex density versus distance into the sample, in terms of unit cells; i.e., $[m(L_x)/L_y - m(0)/L_y]/(L_x-0)$.

[b]Parameters (r, p, q) = (0.1, 5.0, 0.1) as defined in text.

[c]Parameters (0.1, 12.0, 0.1). The lattice constant for b was calculated using the same critical current as for a. In actuality, the larger pinning strength would call for a larger critical current.

III. RESULTS

A. Numerical results obtained from BP model

All of the runs were carried out using $2^{20}\sim 10^6$ time steps. For most choices of parameters and vortex injection rates, it was found that the vortex population quickly reached a steady state of the form predicted by the Bean model.[7,8] That is, the magnetic induction gradient dB/dx from left to right (i.e., in the direction of vortex injection) rapidly approached a constant value (see Table I). According to the Bean model,[9] this constant value is related to the critical current density J_c of the superconductor (see below).

Our goal in this work is to calculate the flux noise produced by vortices falling off the right edge of the sample. This goal is similar to that of Jensen, who has also used a coarse-grained model to study the power spectrum of a self-organized critical state.[10] Jensen's model, however, differs from the BP model in several respects. For example, the Jensen model forbids occupancy of a site by more than one vortex, and it also allows vortices to fall off both the right and left edges of the system. Thus, we expect the two models to give different predictions for noise spectra.

To calculate the flux noise in the present model, we used the following approach. In experiment, the flux noise is measured by placing a detector coil in the center of a hollow sample ring,[6] as shown in Fig. 2. According to Faraday's law, the voltage generated in the coil is proportional to the rate of change of vortex population within the coil area. To display this, we plot in the figures the Fourier transform

$$S_\Phi(f)=\mathrm{Lim}_{T\to\infty}\left|\int_0^T N'(t)\exp(-i2\pi ft)dt\right|^2, \quad (2)$$

where $N'(t)$ represents the rate of change of vortex population in the region to the right of the sample at time t. (Our transverse periodic boundary conditions correspond to a ring geometry.) In our calculations, $N'(t)$ is taken as the number of vortices which fall off the right-hand edge of the sample in a single time step at time t. We evaluate the Fourier trans-

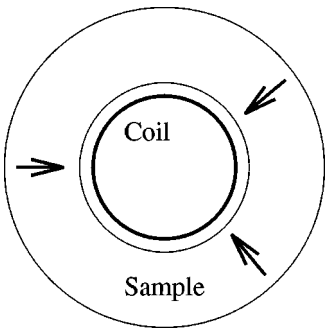

FIG. 2. Schematic of experimental arrangement for noise measurements, as viewed from above. The arrows denote the average direction of vortex motion, under the influence of an increasing external magnetic field applied to the outside of the torus. The coil is used to measure the flux noise.

form using the integral given above, then smooth the resulting power spectrum using a Savitzky-Golay filter as described in Ref. 11. We used first order smoothing over twenty points on either side of the data point.

Our results are shown in Figs. 3 and 4. In general, for all the spectra shown, the power spectrum exhibits a power-law dependence on frequency, over a portion of the frequency range, i.e., $S_\Phi(f) \sim f^{-s}$, resembling that seen in the experimental results of Field *et al.*[6] In Fig. 3, $s \sim 1.0$ for spectra *a*, *b*, and *c*. $s \sim 1.4$ for *d*. In general, *s* is found to increase from 1.0 to 1.4 when the injection rate is reduced below one vortex per time step across the entire left-hand edge. However *s* never achieves the experimentally observed value of ~ 1.5, as seen, for example, in the results of Ref. 6.

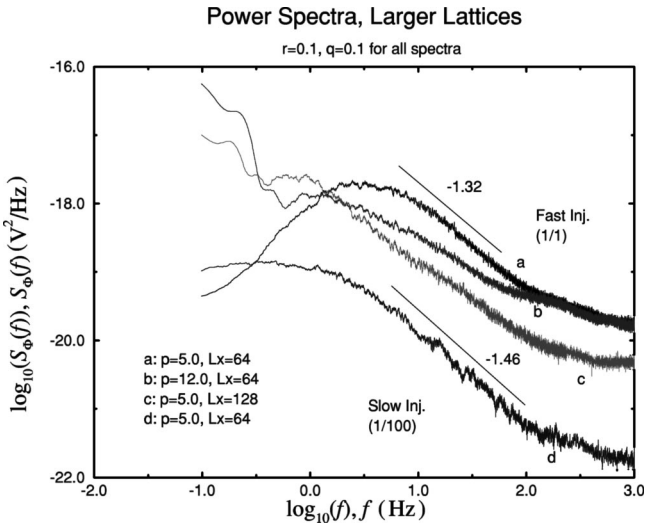

FIG. 3. Calculated voltage noise spectra due to flux motion into the interior of the torus, for several choices of parameters and primarily for larger lattices. *r* and *q* are 0.1 for all spectra. The legend indicates the pinning strength *p* and the lattice width (in units of a_x.) The injection rate is one vortex injected per time step (fast injection) for spectra *a*, *b*, and *c*, and one vortex injected per 100 time steps (slow injection) for spectrum *d*. The numerical data were collected for a run of 2^{20} time steps, using a Savitzky-Golay smoothing filter of order 1, using 40 points. The translation into real frequency is made assuming the estimates of time constant and lattice constant as described in the text.

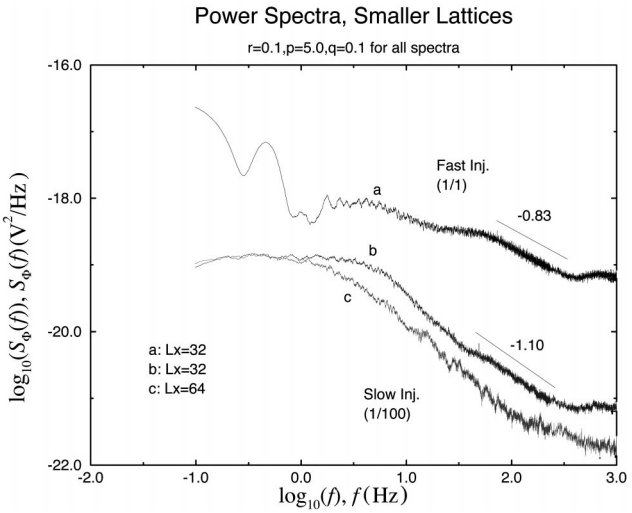

FIG. 4. Additional calculated vortex noise spectra, primarily for smaller lattices. These results show a possible ''knee'' in curve *a*. This curve represents an injection rate of one vortex per time step, which would correspond to experimental data taken at a high rate of vortex injection. This curve should be contrasted to curves *b* and *c*, which are taken at lower rates of magnetic field ramping (1 vortex per 100 times steps) and show no such knee.

For the relatively small lattices $L \leqslant 32$, we often see a characteristic feature in the power spectrum which is missing at larger sizes. Namely, for an injection rate of one vortex per time step, where the vortex can enter anywhere along the left-hand edge, the power spectrum exhibits a plateau; see Fig. 4(a). This plateau disappears as the injection rate is decreased. For example, at an injection rate of 1 vortex per 100 time steps [see Fig. 4(b)], no plateau is apparent. The plateau is due to the emergence of a new length scale in the lattice for small lattices and large injection rates, namely, the smallest linear dimension of the lattice itself. Under such conditions, the lattice size limits the avalanche dimensions. This new length scale in turn produces the high-frequency ''knee'' in the noise spectrum. Specifically, at these frequencies, lattice-wide avalanches dominate, drowning out the high-frequency noise produced by sporadic independent avalanches. As in the other power spectra generated by the model, the calculated slope $b \equiv -d \ln[S_v(\omega)]/d \ln(\omega)$ for frequencies ω above the knee of Fig. 4 is smaller than the experimental value $b_{\rm exp}$; our calculated value in this regime is $b \sim -1$ compared to the experimental value of $b_{\rm exp} \sim -2$.[6]

A vortex injection rate greater than 1/1 (i.e., greater than one vortex per lattice site per time step) was also attempted, so that multiple vortices were randomly injected into the lattice simultaneously. The goal of this test was to check if a ''knee'' could be created at larger length scales at sufficiently high injection rates. But this test resulted in a power spectrum with nearly white noise, i.e., $b \sim 0$. It is possible that, with the rather limited lattice size of $L = 32$, the size of avalanches is inevitably restricted purely by size limitations, whereas in the larger lattices, the vortices exhibit a different avalanche pattern, unconstrained by lattice size.

B. Connection to experiment

In order to compare our model results with the experiments of Field *et al.*, we need to estimate the lattice constant

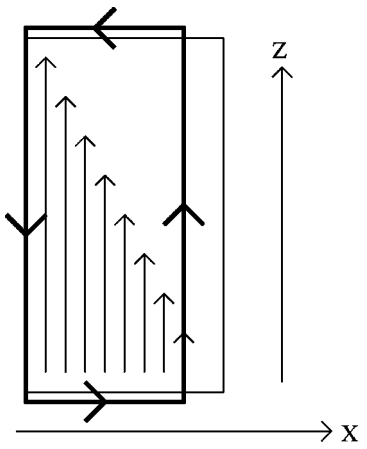

FIG. 5. Cross section of the vortex population in the sample (schematically indicated by the length of the vertical arrows) after the vortex density has relaxed to the steady-state vortex profile, showing the linear decrease in magnetic induction with distance into the sample, as predicted by the Bean model. The path of the line integral used to integrate Ampere's law is shown in boldface.

and time step of the simulation. To obtain the lattice constant, we look at a cross-section of the lattice, as seen in Fig. 5. Then integrating Ampere's law

$$\nabla \times \mathbf{B} = \frac{4\pi}{c}\mathbf{J} \tag{3}$$

along the path in Fig. 5, and assuming a constant current density equal to the critical current density, $J = J_c$ (as expected in the Bean critical state), we find

$$B_z(x) = B_z(0) - \left(\frac{4\pi}{c} J_c\right) x. \tag{4}$$

If we multiply this expression by the area of a narrow vertical strip of the lattice, $(L/4)a_y a_x$, we obtain the flux through the vertical strip centered at x and of width a_x as

$$\Phi(x) = \Phi(0) - \left(\frac{\pi J_c L}{c} a_y a_x\right) x. \tag{5}$$

To proceed further, we write $x = n_x a_x$, where a_x is the distance between two opposite sides of the hexagonal cell (see Fig. 1), and we denote by $m(x)$ the total flux through a column parallel to y, of width a_x, and centered at $n_x a_x$. Then it follows from Eq. 5 that

$$m(n_x) = m(0) - \left(\frac{\pi J_c L}{\Phi_0 c} a_x{}^2 a_y\right) n_x. \tag{6}$$

Finally, if the cells are equilateral hexagons of side a, then $a_x = a\sqrt{3}$ and $a_y = 3a$, and hence

$$m(n_x) = m(0) - \left(\frac{9\pi J_c L a^3}{\Phi_0 c}\right) n_x. \tag{7}$$

We can use this equation to interpret our numerical results for the vortex densities and flux noise spectrum. We also need an estimate of J_c, the critical current density for the sample studied experimentally. In this case, the sample is the composite material $Nb_{0.47}Ti_{0.53}$ (typically in the form of a solid solution with precipitates which constitute the pinning centers). Experiments suggest a value in the range of 3×10^{15} statamperes/cm^2,[12] from which we can estimate a from

$$a = \left(\frac{m(0)\Phi_0 c}{9\pi L^2 J_c}\right)^{1/3}. \tag{8}$$

Some representative values of a, as calculated from our simulations, are shown in Table I.

Once a is determined, the simulation time constant, τ_0, can be estimated by equating the Lorentz force per unit length on a vortex to the pinning force per unit length, i.e.,

$$f_{\text{pin}} = f_L. \tag{9}$$

We assume that f_{pin} can be interpreted as a vortex drag force proportional to the average vortex velocity v, i.e., $f_{\text{pin}} = \eta v$, where η is an effective friction coefficient. Then writing out the Lorentz force on a unit length of a single vortex explicitly gives

$$\eta v = \frac{J\Phi_0}{c}. \tag{10}$$

Now a vortex can move only one lattice constant per time step, so that $v \sim a/\tau_0$. Furthermore, $\eta = B\Phi_0/\rho c^2$, where B is the local magnetic induction, ρ is the flux flow resistivity, and c is the speed of light. Combining these relations gives

$$\tau_0 = \frac{Ba}{\rho c J_c}. \tag{11}$$

If we assume a magnetic induction of 5 kG, a lattice constant of 3.22×10^{-5} cm as suggested by the estimates in Table I, a critical current of 3×10^{15} statamps/cm^2 as is typical for the experiments of Field *et al*, and a flux flow resistivity of 1.11×10^{-23} sec, as suggested by experiments on NbTi alloys,[11] then one obtains a time constant $\tau_0 \sim 2 \times 10^{-4}$ s.

It is of some interest to compare the value of a calculated here with some other characteristic lengths in the superconductor. For a field of around 5 kG, the intervortex spacing a_v of the undistorted lattice is $(\frac{4}{3})^{1/4}\sqrt{\Phi_0/B} = 6.80 \times 10^{-6}$ cm. Thus, each lattice point in the kinetic model would correspond to 25 or more vortices, as is appropriate for this coarse-graining approach. Another characteristic length is the penetration depth λ, a measure of the range of intervortex interaction; for $Nb_{0.47}Ti_{0.53}$, the zero-temperature λ is $\sim 1.83 \times 10^{-5}$ cm.[11] This is somewhat smaller than the lattice constant of the simulation grid, 3.22×10^{-5} cm. Finally, a third length of interest is the so-called Larkin length R_c,[9,13] which is the length beyond which the vortex crystalline order is disrupted by pinning. In the two-dimensional collective pinning model,[13,14] R_c can be written as

$$R_c = \sqrt{\frac{H_{c1} a_v^2 c}{16\pi J_c \xi}}, \tag{12}$$

where H_{c1} is estimated to be 200 G at zero temperature and the zero temperature coherence length ξ is estimated at 3.16×10^{-7} cm.[11] This yields a Larkin length of 7.63 $\times 10^{-5}$ cm. Taken together, these estimates suggest that the

present kinetic approach may be adequate for the system studied experimentally by Field *et al*, since the simulation lattice does have a lattice constant substantially larger than that of the undistorted vortex lattice, while the Larkin length is on the same scale as the simulation lattice constant.

IV. DISCUSSION

If the value of τ_0 found in the previous section is substituted into our calculated frequency spectrum, we find that the spectrum has a power-law frequency dependence over a slightly different frequency range than that in which power-law behavior is seen by Field *et al* in $Nb_{0.47}Ti_{0.53}$ (cf. Figs. 3 and 4). Furthermore, the strength of the model flux noise power is smaller than the experimental values by a factor ranging from two (at high frequencies, for high injection rate) to five (at low frequencies, for low injection rate) orders of magnitude.

These differences between our calculated power spectrum and the measured spectrum are not surprising. The model is a only a rough approximation to a real material, since it uses an artificial kinetics rather than a more realistic (and more computer intensive) dynamics for the calculation. Furthermore, because of the finite size of the simulation samples, they produce significantly less flux noise than would be generated by a real material. Nevertheless, the model does give the qualitatively correct behavior: it leads to a power-law exponent which seems to approach the observed value for a sufficiently low vortex injection rate and a sufficiently large lattice.

The noise spectra deviate from power-law behavior at low frequencies. Specifically, they all show a weak peak at low frequencies, followed by a further decrease with diminishing frequency and finally an increase at still lower frequencies. We believe that this peak occurs near the frequency of a characteristic ''lattice resonance.'' Qualitatively, this frequency is the ratio of a characteristic length, i.e., the linear dimension of the lattice, and a characteristic time, which is the time required for the lattice to ''reload'' to its Bean critical state between avalanches. For a lattice of size $L_x=64$, having pinning parameters (0.1,5.0,0.1) and an injection rate of one vortex per time step, the resonant frequency occurs at about 3 Hz (using our estimates for lattice constant and time step). For the same parameters but slower injection rate (one vortex per $100\tau_0$), the noise spectrum still shows a peak but now at a lower resonance frequency of 0.3 Hz. For other values of the pinning parameters and injection rates, the resonance becomes less conspicuous. The resonant peak also becomes much less conspicuous in a larger lattice. In this case, the lattice simply contains more vortices. Since some of these may not join the primary avalanche, they tend to move separately, reducing the apparent reload time and hence producing a stronger low-frequency noise signal. The same argument holds when the pinning strength is increased at constant lattice size. In this case, there are once again more vortices in the system than at weaker pinning, and hence, a stronger low-frequency flux noise signal. Finally, at high injection rates (e.g., in the $L_x=32$ lattice at an injection rate of one vortex per time step), the vortex system is in a state of continual avalanche motion, since this rate is very large for such a small lattice. As a result, the power spectrum, which reflects that of the avalanches, is relatively flat as a function of frequency.

Finally, we comment briefly on the relation of our calculation to a similar study done by Nori and collaborators.[15] In contrast to our work, their calculations were carried out using dynamical equations for individual vortices (assuming overdamped motion and a particular force law to describe vortex-vortex interactions; the equations were solved using molecular dynamics methods. Their calculations were carried out solely in the slow-driving limit; the resulting noise spectra, similar to those presented here in the slow-driving limit, exhibited a power law in agreement with experiments carried out in that slow-driving regime. But our calculations do have the advantage of speed: a realistic MD model using overdamped dynamics of individual vortices requires approximately 10^4 hours on a machine with parallel processing. By contrast, our power spectra were calculated using a single Digital Alphastation 255 for only 10^2 h. This speed allows us to vary the parameters extensively, in particular examining the effects of different driving rates, which in turn permits investigation of the shoulders in the power spectra mentioned above. Of course, the kinetic approach does have the compensating disadvantage of invoking a drastic simplification to the true equations of motion; but it still appears to preserve much of the relevant physics.

To summarize, we have shown that a relatively simple kinetic model of vortex avalanches near the Bean critical state[1] gives rise to flux noise which qualitatively resembles experiment, without using computer-intensive dynamical equations for individual vortices. Specifically, the model predicts a power law flux noise spectrum with approximately the correct power-law exponents, as well as a length-scale-induced knee in the power spectrum for a sufficiently small lattice at high frequencies. Although the model calculations differ in detail from experimental results, they do show many qualitative similarities and trends in the context of rather simple kinetic equations.

ACKNOWLEDGMENTS

We are grateful for support from the National Science Foundation, Grant No. DMR97-31511, and from the Department of Energy through the Midwest Superconductivity Consortium at Purdue University, Grant No. DE-FG 02-90 ER45427. We also thank F. Nori for valuable conversations.

[1] K.E. Bassler and M. Paczuski, Phys. Rev. Lett. **81**, 3761 (1998).
[2] P. Bak, C. Tang, and K. Wiesenfeld, Phys. Rev. A **38**, 364 (1988).
[3] M. Paczuski, S. Maslov, and P. Bak, Phys. Rev. E **53**, 414 (1996).
[4] R.A. Richardson, O. Pla, and F. Nori, Phys. Rev. Lett. **72**, 1268 (1994); C. Reichhardt, C.J. Olson, J. Groth, S. Field, and F. Nori, Phys. Rev. B **52**, 10 441 (1995).
[5] Obviously, these lattice sites in no way correspond to the sites of any possible Abrikosov lattice.
[6] S. Field, J. Witt, F. Nori, and X. Ling, Phys. Rev. Lett. **74**, 1206 (1995).
[7] C.P. Bean, Phys. Rev. Lett. **8**, 250 (1962).
[8] C.P. Bean, Rev. Mod. Phys. **36**, 31 (1964).
[9] M. Tinkham, *Introduction to Superconductivity* (McGraw-Hill, New York, 1996).
[10] H. Jensen, Phys. Rev. Lett. **64**, 3103 (1990).
[11] W. Press, S. Teukolsky, W. Vetterling, and B. Flannery, *Numerical Recipes* (Cambridge University Press, New York 1992).
[12] E.W. Collings, *Applied Superconductivity, Metallurgy, and Physics of Titanium Alloys* (Plenum, New York, 1986).
[13] A.I. Larkin and Yu.V. Ovchinnikov, J. Low Temp. Phys. **34**, 409 (1979).
[14] See, for example, Chap. 9 of Ref. 9 for a discussion.
[15] C.J. Olson, C. Reichhardt, J. Groth, S. Field, and F. Nori, Physica C **270**, 89 (1997).